

# Exploring Emission Line Variability and Jet-Broad Line Region Interaction in the Blazar TON 599

Jonhatan U. Guerrero-González<sup>1</sup>, Vahram Chavushyan<sup>1</sup> and

Víctor M. Patiño-Álvarez<sup>1,2</sup>

<sup>1</sup> *Instituto Nacional de Astrofísica, Óptica y Electrónica (INAOE), Luis Enrique Erro #1, Tonantzintla, Puebla, México, C.P. 72840*

<sup>2</sup> *Max-Planck-Institut für Radioastronomie, Auf dem Hügel 69, D-53121 Bonn, Germany*

Received: September 26, 2025; Accepted: November 20, 2025

**Abstract.** Blazars, a highly variable Active Galactic Nuclei (AGNs) subclass, provide a unique opportunity to explore the physical processes within their relativistic jets and emission regions. In this study, we investigate the multi-wavelength variability of the blazar TON 599, a Flat Spectrum Radio Quasar (FSRQ), with a particular emphasis on its emission line behavior. We focus on the Mg II  $\lambda 2798$  Å emission line, a key tracer of the ionized gas in the broad-line region (BLR), and its role in jet-induced variability. In addition to optical emission lines, we analyze gamma-rays (0.1–300 GeV), X-rays (0.2–10 keV), optical continuum ( $\lambda 3000$  Å), optical polarization, and millimeter-wavelength light curves. Three cross-correlation methods are employed to investigate temporal relationships between the emission line and continuum across various wavelengths. Using the Non-Thermal Dominance (NTD) parameter, our analysis confirms that synchrotron emission dominates the continuum during active states, highlighting the jet’s primary role in the observed variability. The Mg II emission line exhibits quasi-simultaneous variability with the optical continuum, suggesting photoionization driven by the jet’s non-thermal radiation. Additionally, the minimal time lag between gamma-ray and optical/near-ultraviolet emissions supports a synchrotron self-Compton origin for the most variable component of the gamma-ray emission. These findings highlight the importance of emission line variability and multiwavelength observations in constraining the interaction between jets and the BLR in blazars. The results contribute to a deeper understanding of AGN emission mechanisms and the complex interplay between jets and their surrounding environments.

## 1. Introduction

Supermassive black holes (SMBHs) reside at the centers of most galaxies, and those with high accretion rates give rise to Active Galactic Nuclei (AGN) (Urry & Padovani, 1995). A remarkable subclass of AGN is represented by blazars,

whose relativistic jets are aligned close to our line of sight. They are powerful radio sources, characterized by extreme variability across the entire electromagnetic spectrum, with timescales ranging from years to minutes. Blazars provide a unique laboratory for studying physical conditions that cannot be reproduced on Earth.

Blazars are commonly divided into two subclasses: BL Lacertae objects (BL Lacs) and Flat Spectrum Radio Quasars (FSRQs). In particular, FSRQs tend to show broad optical emission lines (e.g.,  $H\beta$ , Mg II, C IV) in addition to a non-thermal continuum (Urry & Padovani, 1995; Véron-Cetty & Véron, 2000). By contrast, BL Lacs are characterized by optical spectra dominated by a nearly featureless non-thermal continuum with very weak or absent emission lines (Stickel et al., 1991).

Within this context, this work focuses on the blazar TON 599 ( $z = 0.725$ ; Hewett & Wild 2010), classified as an FSRQ. We investigate its multifrequency variability, including gamma rays (0.1–300 GeV), X-rays (0.2–10 keV), the UV spectral continuum (3000 Å), the Mg II  $\lambda 2798$  Å emission line, optical polarization (5000–7000 Å), and 1 mm emissions. Cross-correlation analysis is employed to explore connections among these bands. This study provides new insights into the multifrequency emission processes of TON 599 and contributes to a broader understanding of blazar-type AGN.

## 2. Object of Study

The blazar TON 599 is classified as a Flat Spectrum Radio Quasar (FSRQ) due to its strong broad line emission and small viewing angle, making it one of the most variable types of AGN (Wills et al., 1983; Prince, 2019; Hallum et al., 2022).

Originally discovered in the 1950s by Iriarte & Chavira (1957), TON 599 was included in a catalog of more than 800 “blue stars” identified near the North Galactic Pole, as part of an observational program carried out with the Tonantzintla Schmidt Camera, in Puebla, Mexico. Since then, this source has been extensively monitored by multiple facilities, yielding a rich multi-band archive and numerous publications that consistently confirm its strong variability across different wavelengths.

Figure 1 shows the original identification chart of TON 599 together with its UV/optical spectrum, illustrating both the historical context of its discovery and the spectral features that define it as an FSRQ.

## 3. Methodology

The observations analyzed in this work span multiple wavelengths. Gamma-ray data were obtained from *Fermi*-LAT, while X-ray data were taken from the *Swift*-XRT *Monitoring of Fermi-LAT Sources of Interest*. Optical spectra

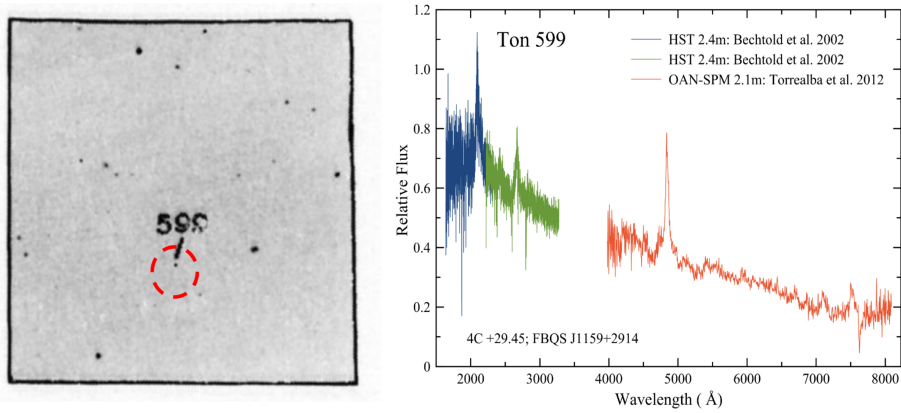


**Figure 1.** Left: Identification chart of TON 599 (Iriarte & Chavira, 1957). Right: Observed frame UV/Optical spectrum of TON 599 (Bechtold et al., 2002; Torrealba et al., 2012)

were retrieved from the database of the Ground-Based Observational Program associated with the *Fermi* Gamma-ray Space Telescope at the University of Arizona, and 1 mm observations were collected from the Submillimeter Array (SMA) database.

In total, 196 spectra of TON 599 were compiled, of which two were discarded due to low signal-to-noise ratio. For each remaining spectrum, a fitting procedure was performed on the Mg II  $\lambda 2798$  Å emission line using multi-component models. The continuum was fitted with a power-law function, the Fe II emission in the UV was modeled with empirical templates (Vestergaard & Wilkes, 2001), and the Mg II line itself was decomposed into broad and narrow components with Gaussian profiles (see Figure 2 for an example of the fitting procedure). This approach allowed us to reliably characterize the spectral features of TON 599.

From these fits we derived integrated fluxes, line and continuum luminosities, and subsequently physical parameters such as the Non-Thermal Dominance (NTD), which are discussed in the following section.

#### 4. Non-Thermal Dominance Parameter: NTD

The non-thermal dominance (NTD) parameter, introduced by Shaw et al. (2012), quantifies the contribution of the relativistic jet to the optical/UV continuum and is defined as:

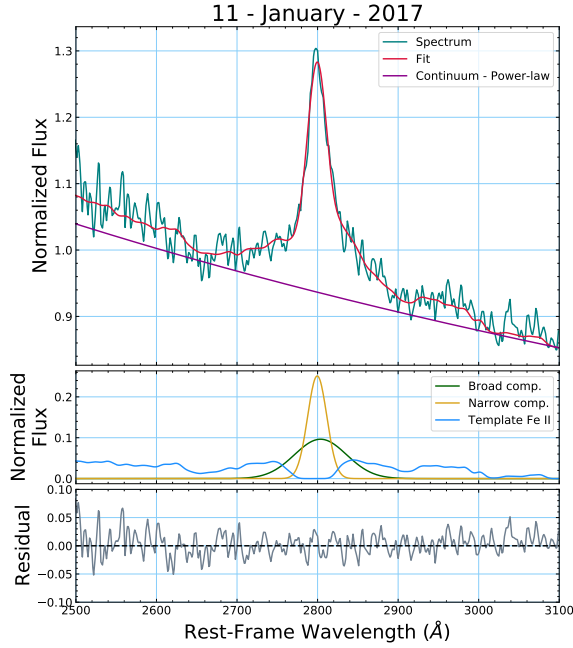


**Figure 2.** Example of a TON 599 spectrum (January 2017, Steward Observatory) showing the multi-component fit and residuals.

$$NTD = \frac{L_{obs}}{L_{pred}}, \quad (1)$$

where  $L_{obs}$  is the observed luminosity and  $L_{pred}$  is the predicted luminosity inferred from emission lines in non-blazar AGNs. Since broad emission lines trace the accretion disk power (i.e.  $L_{pred}=L_{disk}$ ), Patiño Álvarez et al. (2016) reformulated NTD as:

$$NTD = 1 + \frac{L_{jet}}{L_{disk}}, \quad NTD \geq 1, \quad (2)$$

which allows different regimes to be identified:  $NTD = 1$  (only disk emission),  $1 < NTD < 2$  (disk-dominated),  $NTD = 2$  (equal contributions from disk and jet), and  $NTD > 2$  (jet-dominated).

The value of  $L_{pred}$  was obtained from the empirical relation between  $L_{MgII}$  and  $L_{3000 \text{ \AA}}$  derived from a sample of  $\sim 40,000$  radio-quiet AGN (Patiño-Álvarez et al., 2025) :

$$\log L_{MgII} = (0.826 \pm 0.025) \log \lambda L_{\lambda 3000} + (6.057 \pm 1.164). \quad (3)$$

Here,  $L_{MgII}$  was measured from the integrated flux of the emission line, while  $L_{obs}$  was derived from the continuum flux at  $3000 \text{ \AA}$ , both calculated using a luminosity distance of  $D_L = 4445.5 \text{ Mpc}$  ( $z = 0.725$ ).

In addition, single-epoch black hole mass estimates were obtained using standard virial relations based on the Mg II emission line luminosity and the  $3000 \text{ \AA}$  continuum (Kong et al., 2006; Vestergaard & Peterson, 2006; Shen et al., 2011). These methods assume that the Broad Line Region (BLR) is virialized and that the continuum is primarily powered by the accretion disk.

For jet-dominated sources such as TON 599, however, the continuum can be significantly contaminated by non-thermal emission, which may lead to systematic overestimations of  $M_{BH}$ . Since the Mg II emission line is expected to be less affected by this contamination, mass estimates derived from  $L_{MgII}$  are considered more reliable in these cases. Figure 3 shows the relation between  $L_{MgII}$  and  $L_{3000 \text{ \AA}}$  for TON 599, where deviations from the empirical trend directly reflect the increasing jet contribution and its impact on black hole mass determinations.

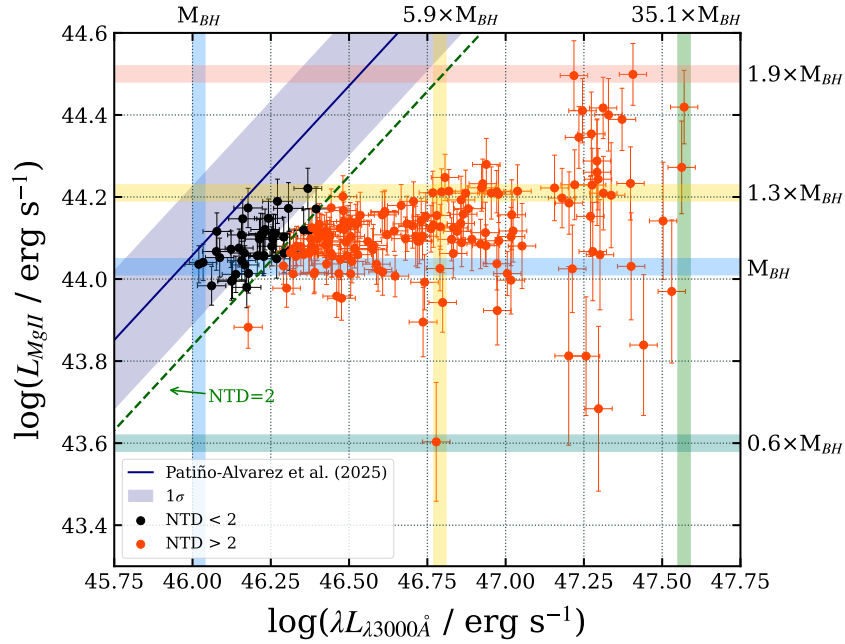


**Figure 3.** Variations in the Mg II emission line luminosity versus the continuum luminosity at  $3000 \text{ \AA}$  for TON 599. The right and top axes show overestimations and underestimations of the black hole mass when calculated using single-epoch techniques, using the continuum and emission line luminosity, respectively.

## 5. Cross-Correlation Analysis

To investigate possible time lags between the continuum and emission line variability, we applied cross-correlation functions (CCFs) using three complementary approaches: the interpolated CCF (Gaskell & Sparke, 1986), the discrete CCF (Edelson & Krolik, 1988), and the Z-transformed DCF (Alexander, 1997), all incorporating non-stationarity corrections (Patiño-Álvarez et al., 2013; Amaya-Almazán et al., 2022).

The statistical significance of the correlations was evaluated through Monte Carlo simulations (Timmer & Koenig, 1995; Emmanoulopoulos et al., 2013), with confidence levels at 90, 95, and 99% (grey lines in Figure 4). In this work, we adopt the 99% level as the threshold for reliable correlations. Employing multiple CCF methods enhances robustness by mitigating the effects of interpolation gaps, spurious peaks, and aliasing, among other caveats the data might present.

As an illustrative example, Figure 4 presents the results of the cross-correlation between the gamma-ray and 3000 Å light curves using the three methods, illustrating both the consistency of the techniques and the regions where significant correlations are detected. In this figure, we see that the ICCF does not exceed the 99% confidence level, whereas the DCCF and ZDCF show a significant correlation within the same lag range. This difference stems from the ICCF's sensitivity to interpolation and irregular sampling. Therefore, for this specific case we consider the detection supported by DCCF/ZDCF to be more reliable.

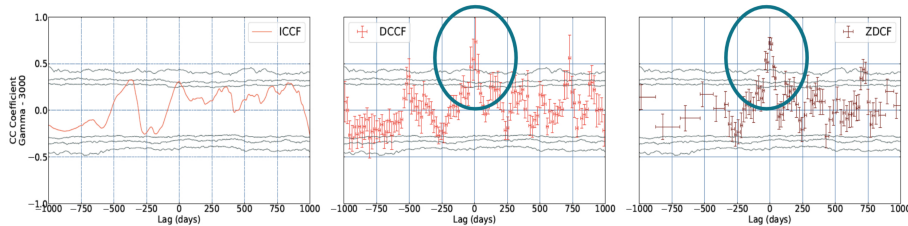


**Figure 4.** Example of the cross-correlation functions; in this case between the gamma-ray and 3000 Å light curves using three methods. Left: interpolated cross-correlation function (ICCF); middle: discrete cross-correlation function (DCCF); right: Z-transformed discrete correlation function (ZDCF).

## 6. Results

The results presented below are derived from a joint analysis of the multi-frequency light curves and the cross-correlations between bands. In particular, the cross-correlations provide information on the time lags between different wavelength bands of the electromagnetic spectrum, which may be related to distances between emitting regions, provided that factors such as the jet viewing angle and the wavelengths involved are taken into account.

Figure 5 shows the multi-frequency light curves of TON 599, including *Fermi*-LAT  $\gamma$  rays (0.1–300 GeV), *Swift*-XRT X rays (0.3–10 keV), optical data from the *Steward Observatory* (4000–7000 Å in the observer’s frame), comprising the rest-frame 3000 Å continuum, the Mg II  $\lambda$ 2798 Å line flux, *V*-band photometry, the polarization degree, and the polarization angle (measured between 5000 and 7000 Å), SMA 1 mm emission, and the Non-Thermal Dominance (NTD) curve computed from the 3000 Å continuum and the Mg II line.

Consistent with the cross-correlation analysis, the *V* band and the 3000 Å continuum vary quasi-simultaneously, with contemporaneous rises and declines in Figure 5 (panels c,e). The NTD in panel (i) increases over the same intervals to values above 2 (black dashed line), indicating enhanced jet contribution. The  $\gamma$ -ray activity (panel a) rises during the main optical/NUV events, in agreement with the significant correlations recovered by the discrete and *Z*-transformed discrete correlation functions. The Mg II  $\lambda$ 2798 Å emission line (panel d) exhibits flux enhancements that coincide with optical/NUV high states, consistent with near-zero lags found for the line–continuum pairs.

By contrast, some bands do not show clear correlations. The X-ray coverage (panel b) is limited and does not sample the strongest optical/NUV outbursts, which restricts any association. The 1 mm emission (panel f) traces longer variability timescales and lacks dense sampling during the short optical/NUV flares, reducing the expected cross-correlation signal. The polarization degree and polarization angle (panels g–h) show variability but no consistent temporal relation with the other bands in this dataset. Finally, the  $\gamma$ -ray–Mg II correlation is inconclusive, mainly due to cadence and sampling differences between the high-energy and emission line light curves.

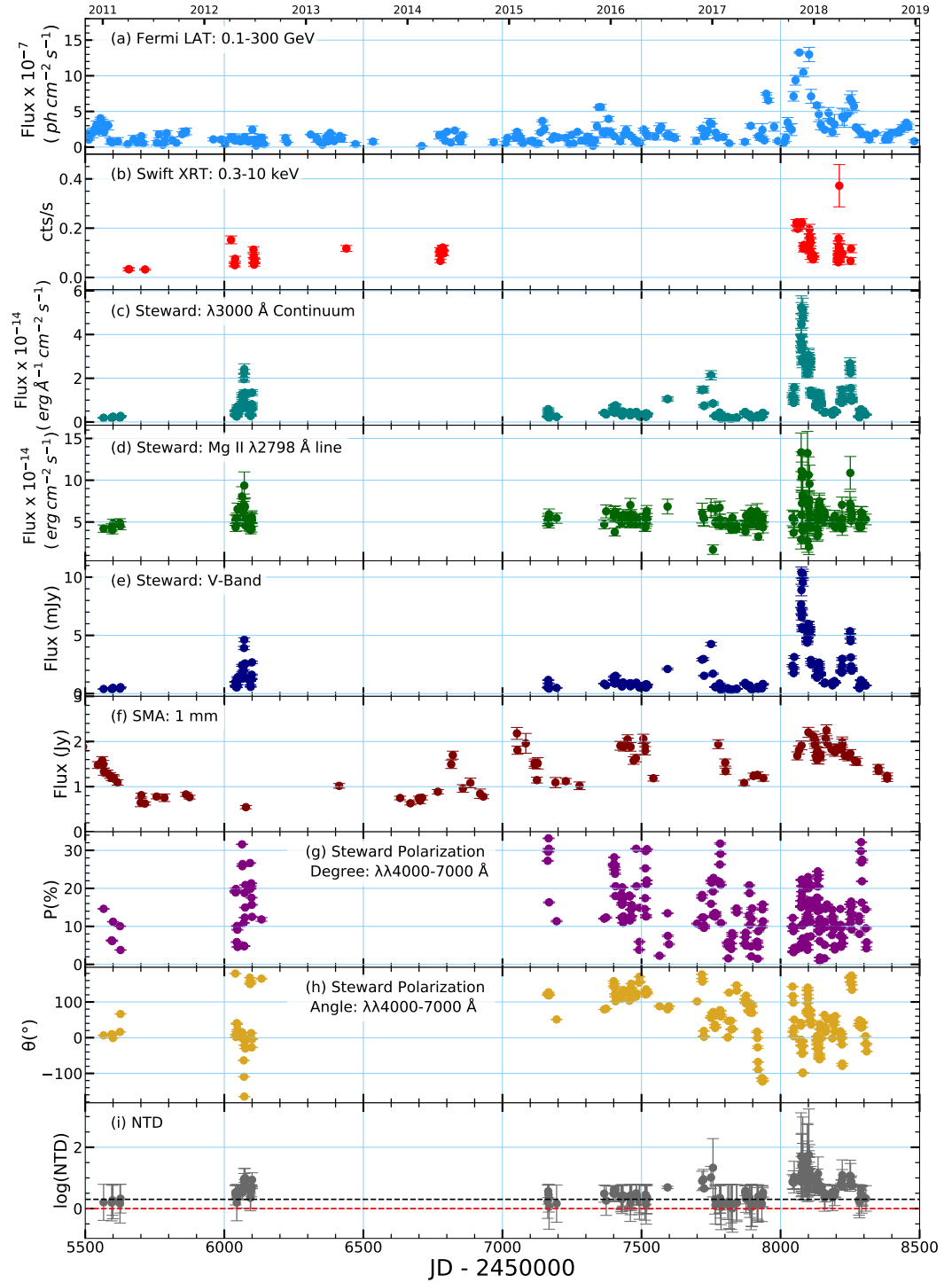


Figure 5. Multifrequency Light Curves for TON 599.

## 7. Conclusions

The cross-correlation analysis and multifrequency monitoring of TON 599 allow us to identify several key results regarding the connection between the jet, the optical/UV continuum, the emission lines, and the high-energy emission. These findings can be summarized as follows:

1. The cross-correlations between the  $V$  band, the 3000 Å continuum, and the NTD are consistent with zero lag. This indicates co-spatiality among the optical/NUV emissions, with the main variability in NTD arising from the jet. The similar variability patterns observed in both the  $V$  band and the 3000 Å continuum support the interpretation that these bands are dominated by synchrotron radiation from the jet.
2. The correlations between the optical/NUV bands and gamma rays suggest that the seed photon population is dominated by synchrotron emission, and that the gamma-ray variability is mainly produced by the Synchrotron Self-Compton (SSC) process during high states of the source. This finding that SSC dominates challenges the standard external Compton scenario and has implications for jet models and Spectral Energy Distribution (SED) studies.
3. Cross-correlations between the optical/NUV bands and the Mg II  $\lambda 2798$  Å emission line also yield a zero lag. The temporal coincidence of line flares with optical/NUV variability implies that the line-emitting gas is being ionized by synchrotron radiation from the jet, in addition to the accretion disk.
4. The observed relation between continuum and line luminosities deviates from expectations for a radio-quiet BLR, indicating that the emission line is not solely ionized by the accretion disk. As a result, black hole mass estimates based on single-epoch methods should preferentially use epochs when the continuum is disk-dominated to obtain more realistic values.

Overall, TON 599 demonstrates that optical/NUV synchrotron emission drives both  $\gamma$ -ray SSC variability and Mg II ionization, revealing a strong interplay between the relativistic jet and the BLR. This challenges canonical reverberation mapping assumptions and adds further evidence, consistent with sources such as 3C 454.3 (León-Tavares et al., 2013; Amaya-Almazán et al., 2021), 3C 279 (Patiño-Álvarez et al., 2018), and CTA 102 (Chavushyan et al., 2020), that BLR gas can be directly influenced by jets.

The case of TON 599 highlights how jet-BLR interactions significantly impact both variability patterns and black hole mass determinations in FSRQs. Future efforts should focus on short-timescale flares, testing the NTD threshold across different bands, refining Mg II-based mass estimates with improved instrumental corrections, and extending this methodology to a larger sample of blazars (Massaro et al., 2015).

**Acknowledgements.** This work has been supported by the SECIHTI program during my doctoral studies. Support was also provided by the MPIfR-Mexico Max Planck Partner Group, led by Dr. Víctor Manuel Patiño Álvarez, whose significant contribution to this research is greatly appreciated.

## References

- Alexander, T., Is AGN Variability Correlated with Other AGN Properties? ZDCF Analysis of Small Samples of Sparse Light Curves. 1997, in *Astrophysics and Space Science Library*, Vol. **218**, *Astronomical Time Series*, ed. D. Maoz, A. Sternberg, & E. M. Leibowitz, 163
- Amaya-Almazán, R. A., Chavushyan, V., & Patiño-Álvarez, V. M., Multiwavelength Analysis and the Difference in the Behavior of the Spectral Features during the 2010 and 2014 Flaring Periods of the Blazar 3C 454.3. 2021, *Astrophysical Journal*, **906**, 5, DOI:10.3847/1538-4357/abc689
- Amaya-Almazán, R. A., Chavushyan, V., & Patiño-Álvarez, V. M., Multiwavelength Analysis and the C IV  $\lambda 1549$  Å Emission Line Behavior From 2008 to 2020 of FSRQ B2 1633+382. 2022, *Astrophysical Journal*, **929**, 14, DOI:10.3847/1538-4357/ac5741
- Bechtold, J., Dobrzycki, A., Wilden, B., et al., A Uniform Analysis of the Ly $\alpha$  Forest at  $z = 0-5$ . III. Hubble Space Telescope Faint Object Spectrograph Spectral Atlas. 2002, *Astrophysical Journal, Supplement*, **140**, 143, DOI:10.1086/342489
- Chavushyan, V., Patiño-Álvarez, V. M., Amaya-Almazán, R. A., & Carrasco, L., Flare-like Variability of the Mg II  $\lambda 2798$  Å Emission Line and UV Fe II Band in the Blazar CTA 102. 2020, *Astrophysical Journal*, **891**, 68, DOI:10.3847/1538-4357/ab6ef6
- Edelson, R. A. & Krolik, J. H., The Discrete Correlation Function: A New Method for Analyzing Unevenly Sampled Variability Data. 1988, *Astrophysical Journal*, **333**, 646, DOI:10.1086/166773
- Emmanoulopoulos, D., McHardy, I. M., & Papadakis, I. E., Generating artificial light curves: revisited and updated. 2013, *Monthly Notices of the RAS*, **433**, 907, DOI:10.1093/mnras/stt764
- Gaskell, C. M. & Sparke, L. S., Line Variations in Quasars and Seyfert Galaxies. 1986, *Astrophysical Journal*, **305**, 175, DOI:10.1086/164238
- Hallum, M. K., Jorstad, S. G., Larionov, V. M., et al., Emission-line Variability during a Nonthermal Outburst in the Gamma-Ray Bright Quasar 1156+295. 2022, *Astrophysical Journal*, **926**, 180, DOI:10.3847/1538-4357/ac4710
- Hewett, P. C. & Wild, V., Improved redshifts for SDSS quasar spectra. 2010, *Monthly Notices of the RAS*, **405**, 2302, DOI:10.1111/j.1365-2966.2010.16648.x
- Iriarte, B. & Chavira, E., Estrellas Azules en el Casquete Galactico NorteEstrellas Azules en el Casquete Galactico NorteBlue Stars in the North Galactic Cap. 1957, *Boletín de los Observatorios Tonantzintla y Tacubaya*, **2**, 3

- Kong, M.-Z., Wu, X.-B., Wang, R., & Han, J.-L., Estimating Black Hole Masses of AGNs using Ultraviolet Emission Line Properties. 2006, *Chinese Journal of Astronomy and Astrophysics*, **6**, 396, DOI:10.1088/1009-9271/6/4/02
- León-Tavares, J., Chavushyan, V., Patiño-Álvarez, V., et al., Flare-like Variability of the Mg II  $\lambda$ 2800 Emission Line in the  $\Gamma$ -Ray Blazar 3C 454.3. 2013, *Astrophysical Journal, Letters*, **763**, L36, DOI:10.1088/2041-8205/763/2/L36
- Massaro, E., Maselli, A., Leto, C., et al., The 5th edition of the Roma-BZCAT. A short presentation. 2015, *Astrophysics and Space Science*, **357**, 75, DOI:10.1007/s10509-015-2254-2
- Patiño-Álvarez, V., Carramiñana, A., Carrasco, L., & Chavushyan, V., A Multiwavelength Cross-Correlation Variability Study of Fermi-LAT Blazars. 2013, *arXiv e-prints*, arXiv:1303.1898, DOI:10.48550/arXiv.1303.1898
- Patiño Álvarez, V., Torrealba, J., Chavushyan, V., et al., Baldwin Effect and Additional BLR Component in AGN with Superluminal Jets. 2016, *Frontiers in Astronomy and Space Sciences*, **3**, 19, DOI:10.3389/fspas.2016.00019
- Patiño-Álvarez, V. M., Fernandes, S., Chavushyan, V., et al., Multiwavelength photometric and spectropolarimetric analysis of the FSRQ 3C 279. 2018, *Monthly Notices of the RAS*, **479**, 2037, DOI:10.1093/mnras/sty1497
- Patiño-Álvarez, V. M., Guerrero-González, J. U., Chavushyan, V., et al., The Relationship Between Emission Line and Continuum Luminosity and the Baldwin Effect in Blazars. I. The Case of the Mg II  $\lambda$ 2798 Å Emission Line. 2025, *arXiv e-prints*, arXiv:2511.15695, DOI:10.48550/arXiv.2511.15695
- Prince, R., Multi-frequency Variability Study of Ton 599 during the High Activity of 2017. 2019, *Astrophysical Journal*, **871**, 101, DOI:10.3847/1538-4357/aaf475
- Shaw, M. S., Romani, R. W., Cotter, G., et al., Spectroscopy of Broad-line Blazars from 1LAC. 2012, *Astrophysical Journal*, **748**, 49, DOI:10.1088/0004-637X/748/1/49
- Shen, Y., Richards, G. T., Strauss, M. A., et al., A Catalog of Quasar Properties from Sloan Digital Sky Survey Data Release 7. 2011, *Astrophysical Journal, Supplement*, **194**, 45, DOI:10.1088/0067-0049/194/2/45
- Stickel, M., Padovani, P., Urry, C. M., Fried, J. W., & Kuehr, H., The Complete Sample of 1 Jansky BL Lacertae Objects. I. Summary Properties. 1991, *Astrophysical Journal*, **374**, 431, DOI:10.1086/170133
- Timmer, J. & Koenig, M., On generating power law noise. 1995, *Astronomy and Astrophysics*, **300**, 707
- Torrealba, J., Chavushyan, V., Cruz-González, I., et al., Optical Spectroscopic Atlas of the MOJAVE/2cm AGN Sample. 2012, *Revista Mexicana de Astronomía y Astrofísica*, **48**, 9, DOI:10.48550/arXiv.1107.3416
- Urry, C. M. & Padovani, P., Unified Schemes for Radio-Loud Active Galactic Nuclei. 1995, *Publications of the ASP*, **107**, 803, DOI:10.1086/133630

- Véron-Cetty, M. P. & Véron, P., The emission line spectrum of active galactic nuclei and the unifying scheme. 2000, *Astronomy and Astrophysics Reviews*, **10**, 81, DOI: [10.1007/s001590000006](https://doi.org/10.1007/s001590000006)
- Vestergaard, M. & Peterson, B. M., Determining Central Black Hole Masses in Distant Active Galaxies and Quasars. II. Improved Optical and UV Scaling Relationships. 2006, *Astrophysical Journal*, **641**, 689, DOI: [10.1086/500572](https://doi.org/10.1086/500572)
- Vestergaard, M. & Wilkes, B. J., An Empirical Ultraviolet Template for Iron Emission in Quasars as Derived from I Zwicky 1. 2001, *Astrophysical Journal, Supplement*, **134**, 1, DOI: [10.1086/320357](https://doi.org/10.1086/320357)
- Wills, B. J., Pollock, J. T., Aller, H. D., et al., The QSO 1156+295 : a multifrequency study of recent activity. 1983, *Astrophysical Journal*, **274**, 62, DOI: [10.1086/161426](https://doi.org/10.1086/161426)